Article

A Theoretical Terahertz Metamaterial Absorber Structure with a High Quality Factor Using Two Circular Ring Resonators for Biomedical Sensing

Sagnik Banerjee [1], Uddipan Nath [1], Purba Dutta [1], Amitkumar Vidyakant Jha [1], Bhargav Appasani [1,*] and Nicu Bizon [2,3,4,*]

[1] Kalinga Institute of Industrial Technology, Bhubaneswar 751024, India; 1804044@kiit.ac.in (S.B.); 1830143@kiit.ac.in (U.N.); 1804036@kiit.ac.in (P.D.); amit.jhafet@kiit.ac.in (A.V.J.)
[2] Faculty of Electronics, Communication and Computers, University of Pitesti, 110040 Pitesti, Romania
[3] ICSI Energy, National Research and Development Institute for Cryogenic and Isotopic Technologies, 240050 Ramnicu Valcea, Romania
[4] Doctoral School, Polytechnic University of Bucharest, 313 Splaiul Independentei, 060042 Bucharest, Romania
[*] Correspondence: bhargav.appasanifet@kiit.ac.in (B.A.); nicu.bizon@upit.ro (N.B.)

Abstract: Metamaterial absorbers, on account of their inherent property of electromagnetic radiation absorption, have become a center of attraction for many researchers in recent times. This paper proposes a unique design of a terahertz metamaterial absorber that can be used to sense biomedical samples. The proposed design consists of two identical circular ring resonators (CRRs) made of aluminum on top of a gallium arsenide (GaAs) substrate. On account of its high field confinement in the sensing regime, a near-to-perfect absorption rate of 99.50% is achieved at a frequency of 2.64 THz, along with a large quality factor (Q-Factor) of 44. The design is highly sensitive to the refractive index changes in the encompassing medium. Hence, the proposed absorber can be used as a refractive index sensor exhibiting a reasonable sensitivity of 1500 GHz/RIU and a figure of merit (FoM) of 25. The refractive index range has been varied in the range of 1.34 to 1.39. As many biomedical samples, including cancerous cells, reside within this range, the proposed sensor can be used for biomedical sensing applications.

Keywords: metamaterials; polarization; terahertz; refractive-index sensor; biomedical sensing

1. Introduction

Metamaterials are artificially fabricated composite structures deriving their exotic properties, such as negative permittivity, negative refractive index, optical magnetism, and anomalous reflection, from an internal micro-structure, instead of a chemical composition endowed with natural materials [1,2]. Metamaterial absorbers are essentially a branch of these structures, capable of absorbing the incident electromagnetic radiation. The design of these structures has evolved into a major research area due to their countless applications in various frequency bands [3,4]. In particular, metamaterial absorbers in the terahertz spectrum or terahertz metamaterial absorbers (TMAs) have tremendous applications in biomedical sensing and biomedical imaging [5,6]. T. J. Yen et al. demonstrated a kind of TMA for the first time [7]. In a TMA, the absorption peaks can be tuned or shifted by changing a particular parameter and hence can be utilized in various sensing applications [8]. A biosensor was designed in [9] to compute the thickness of thin films that could attain a sensitivity of 4.05×10^{-2} GHz/nm, based on silicon nitride substrate. Temperature sensors were designed in [10,11], where the absorption spectra of the structure shift with the temperature change. Apart from thickness and temperature sensing, TMAs can also be used to sense the refractive index of the surrounding medium. A refractive index sensor using TMA was designed in [12] which possessed a sensitivity of 163 GHz/RIU

along with a quality factor (Q-factor) of 7.036 and figure of merit (FoM) of 2.67. A TMA-based biosensor was proposed in [13] that consisted of four identical resonators in a single unit cell. The sensitivity of the sensor was 85 GHz/RIU. In [14], another refractive index sensor was proposed that offered a sensitivity of 300 GHz/RIU. The design consisted of a defective square ring resonator on a Teflon dielectric spacer. Table 1 summarizes the various designs proposed by the researchers for measuring the refractive index of the surrounding medium.

Table 1. Comparison of the sensing performance between the proposed absorber and the existing absorbers operating at terahertz frequency regime.

Ref. No.	Q-Factor	FOM	Range of Refractive Index	Step Size (RIU)
[12]	7.036	2.67	$n = 1.0$–1.8	0.2
[13]	8.5	0.85	$n = 1.0$–2.0	0.2
[14]	5.5	0.4	$n = 1.0$–1.4	0.1
[15]	11.6	2.3	$n = 1.0$–1.8	0.1
[16]	40.1	11.75	$n = 1.0$–1.8	0.1
[17]	41.02	6.56	$n = 1.0$–1.6	0.1
[18]	15	3	$n = 1.0$–2.0	0.2
[19]	7	0.5	$n = 1.0$–4.0	1.0
[20]	40	1.5	$n = 1.1$–2.5	0.2
[21]	22.1	2.94	$n = 1.35$–1.39	0.01
[22]	58	7.5	$n = 1.1$–1.6	0.2
[23]	35.36	94.05	$n = 1.0$–1.05	0.01
[24]	15	3	$n = 1.0$–2.0	0.2
[25]	32.167	6.015	$n = 1.0$–1.9	0.3
This paper	44	25	$n = 1.34$–1.39	0.005

Biomedical samples have refractive indices in the range of 1.3 to 1.39 [21]. In particular, bio-samples, such as blood, T-cell-leukemia-infected blood, and cancerous basal cells, have refractive indices in the range of 1.35 to 1.39. Thus, designing a sensor operating in this range with high sensitivity and high resolution can be highly beneficial for diagnosing leukemia, cancer, etc. Most of the works reported in the literature, summarized in Table 1, have demonstrated the sensing of a refractive index in the range of 1 to 1.1. The recent work of Wang et al. proposes a dual square ring resonator with a Q-factor of 296.3 [26]. However, this structure has been demonstrated as sensing refractive indexes from 1 to 1.1. Although designs have been reported as having better Q-factor and FoM than the proposed work, they have not been designed for sensing bio-medical samples. The designs developed for biomedical sensing suffer from a low Q-factor or a low FoM. Additionally, the resolution of these sensors is low. In this paper, a novel refractive index sensor is proposed for biomedical sensing. It is simulated for various refractive indexes in the range of 1.34 to 1.39, and it is observed that the structure offers a sensitivity of 1500 GHz/RIU. A step size of 0.005 RIU is taken for simulating the design. The design consists of two identical circular ring resonators (CRRs) placed adjacent to one another. The structure has a high Q-factor of 44 and FoM of 25.

The paper's organization is as follows: the proposed sensor's structural design is presented in the next section, while the simulation results are reported in Section 3. An elaborate discussion of the appearance of absorption peaks is presented in Section 4 using the current distribution plots. Additionally, a parametric analysis is carried out to justify the choice of the parameters, and finally Section 4 deals with the conclusion.

2. Methods and Materials

The unit cell of the proposed sensor is shown in Figure 1. The top and bottom metal of the proposed structure is aluminum, and the dielectric spacer used is gallium arsenide (GaAs) due to its wider bandgap and higher resistivity. GaAs, a compound semiconductor, has a permittivity of 12.94, and its loss tangent is 0.006. Its thickness has been taken as

h = 6 μm. The top aluminum layer has a thickness of b = 0.4 μm, and it consists of two circular patches of radius r = 23 μm. CRRs and split ring resonators (SRRs) are widely used to design THz metamaterial absorbers [27].
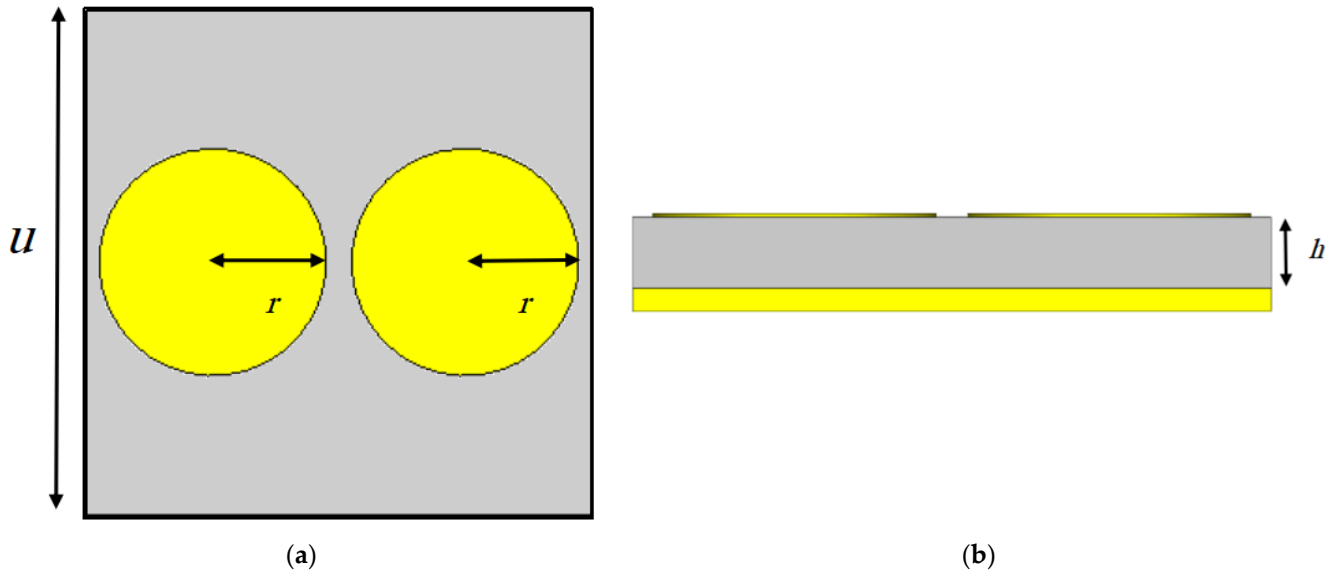

(a)　　　　　　　　　　　　　　　　　　　　　　　　　　　　(b)

Figure 1. Proposed structure of TMA: (**a**) top view; (**b**) side view.

The bottom aluminum sheet has a thickness of t = 2 μm. The bottom layer is taken as sufficiently thick to prevent the transmission of electromagnetic waves. The conductivity of aluminum is taken as 3.56 × 10^7 S/m. The length of the unit cell is 100 μm. Thus, the geometrical specifications of the proposed design are: u = 100 μm, r = 23 μm, t = 2 μm, b = 0.4 μm, and h = 6 μm. Most of the existing metamaterial-based sensors use gold for designing the top and bottom metallic planes. The proposed design uses aluminum instead of gold as it is less expensive, being the most abundant metal on earth. It has a much lighter weight as well as higher malleability and ductility properties when compared to gold. Periodic boundary conditions are applied along the x and y-axes, and the plane wave is incident along the z-axis [28].

3. Results and Analysis

The numerical simulation and design of the structure have been accomplished using the CST Microwave Studio software. In order to devise an apt or efficient terahertz metamaterial absorber, eliminating the transmission and reflection of the incident plane wave is required, thus capitalizing the reciprocity of the absorber with that of the encroaching radiation. The absorption of the structure is determined by Equation (1) [29].

$$A_x = 1 - T_x - R_x \tag{1}$$

where A_x, T_x and R_x represent the coefficients of absorption, transmission, and reflection, respectively. Since the ground metal plane does not allow the transmission of electromagnetic waves, the value of T_x is zero. R_x can also be equalized to zero by designing the top plane properly. Zero values of the transmission coefficient and reflection coefficient indicate that the metamaterial can achieve near-to-perfect absorption. The absorption spectrum of the proposed design is shown in Figure 2a. The proposed design offers a peak absorption of 99.5% at 2.64 THz. In order to check the feasibility of the sensor for practical applications, the absorption spectrum of the absorber is plotted for various angles of polarization in the range of 0° to 45°, as shown in Figure 2b, by considering the normal incidence of the incoming plane wave. It can be seen that all the absorption peaks possess a higher absorption rate of above 95%. There is a minor lateral shift in the absorption

peaks within the spectrum when the polarization angle increases by a considerable amount. Although the proposed sensor is not purely polarization-insensitive, it is seen to provide substantial tolerance up to an angle of polarization of 45°, and hence the sensor can be used in practical applications [30].
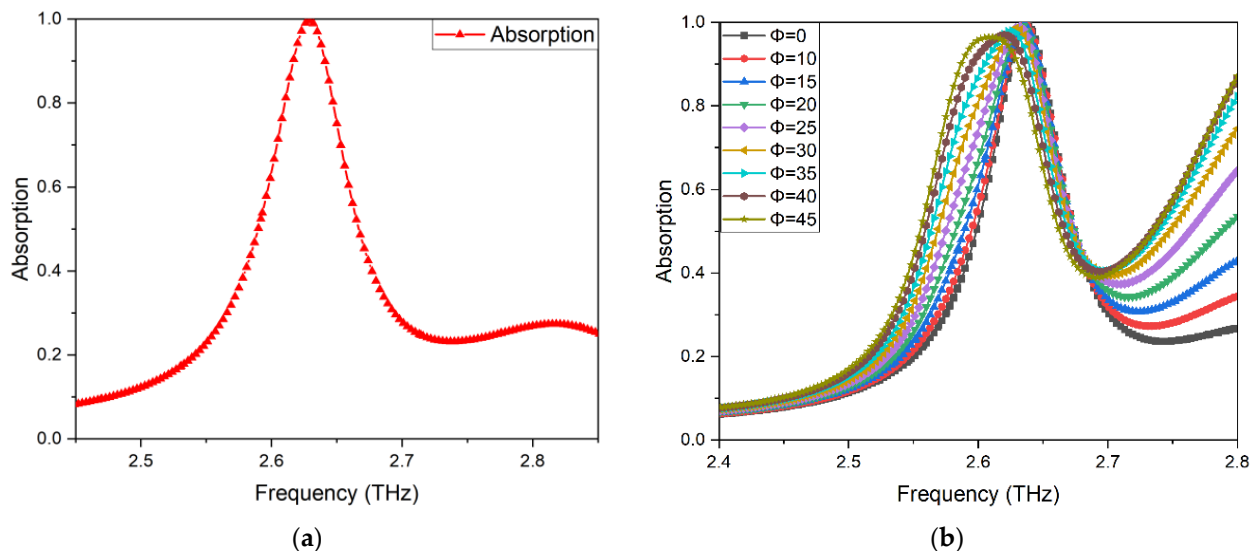

Figure 2. The absorption spectrum of the proposed TMA (**a**) for 0° polarization; (**b**) for other polarization angles.

The absorption peak occurs at 2.64 THz. The suggested design's full-width half maximum (FWHM) is found to be 0.06 THz [31]. This results in a very high-frequency selectivity on account of the extremely narrow absorption bandwidth. Moreover, the quality factor (Q-factor) of any material is defined as the ratio of the resonance frequency to the FWHM. A high Q-factor is always desirable for designing sensors. In the proposed design, the Q-factor was found to be 44, and thus, it is very useful in sensing applications. A single CRR of the same dimension was designed and simulated to justify using two identical CRRs in a single cell. The unit cell of a single CRR and its absorption characteristics are shown in Figure 3.
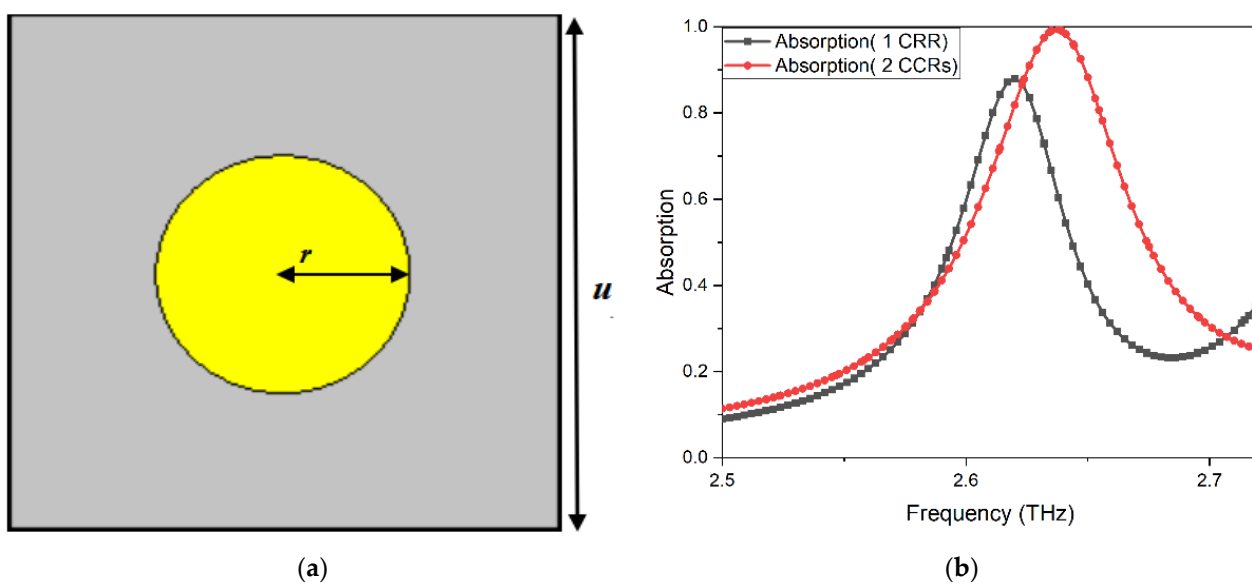

Figure 3. (**a**) Proposed absorber with single CRR; (**b**) comparison of the absorption spectrum for design with single and double CRRs.

A resonating structure is used at the top of a metamaterial absorber in order to couple the incident waves with the surface of the absorber, which leads to absorption. The CRR is responsible for the absorption peaks at the resonant frequency—the larger the CRR, the lower the frequency at which resonance occurs. Figure 3b clearly shows that we obtain nearly perfect absorption using two identical CRRs in the design as the effective surface area of the top surface exposed to the incident light increases, enhancing the coupling phenomenon. Using a single CRR significantly reduces the absorption, which is the motive for using two identical CRRs in the design. Table 2 delineates the performance comparison for both cases.

Table 2. Performance comparison for design with single and double CRRs.

Type of Design	Resonant Frequency	Absorption Rate	FWHM	Quality Factor
2 CRRs	2.64 THz	99.50%	0.06 THz	44
1 CRR	2.62 THz	87%	0.065 THz,	40.30

The proposed design easily outperforms the design with a single CRR. A similar design methodology has been reported in [26] that uses two identical rectangular patches made of gold. Although it manages to attain a sensitivity of 1.9 THz/RIU, it cannot be used as a biomedical sensor as it operates in a range of 1.00 to 1.10. Additionally, the use of gold makes it more expensive than the proposed design. The current distribution plot, which is responsible for the occurrence of the absorption phenomenon, has been represented in Figure 4
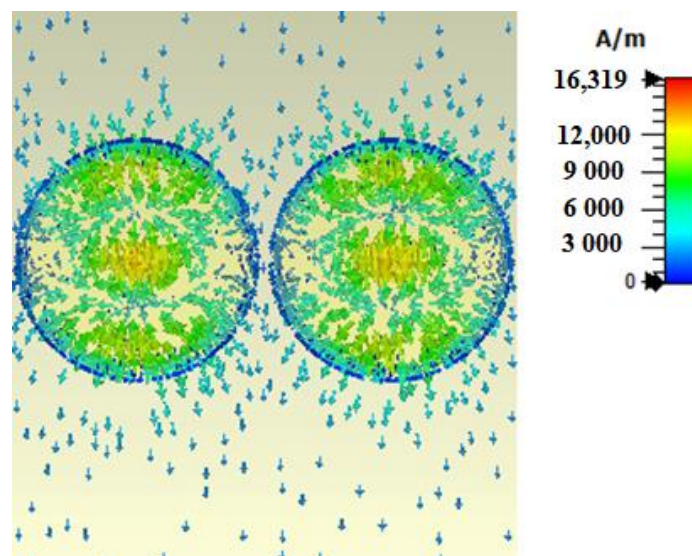

Figure 4. Distribution of surface current at 2.64 THz.

It can be observed that the current distribution pattern is identical in both CRRs. The concentration of current is very high in the interior of the CCRs. There is no significant current distribution at the edges or dielectric, indicating that the resonance is due to the CRRs.

A parametric analysis is provided in Figure 5 to rationalize or justify the design parameters. From the three parts of Figure 5, it is evident that on increasing the value of the parameter (*h*, *u*, and *r*), the resonant frequency decreases, and vice versa. Hence, we obtain an inversely proportional phenomenon. Figure 5a shows that the maximum absorption of 99.5% is achieved for $h = 6$ μm. Increasing or decreasing the height of the substrate reduces the peak absorption. The structure can absorb electromagnetic radiation when the input impedance of the structure matches the free space impedance, i.e., 377 Ω [32]. Increasing or decreasing the substrate thickness disturbs the impedance matching, and

so a 6μm thick substrate, at which the peak absorption is the maximum, is taken. This indicates that for this height, the impedance of the absorber is close to the free space impedance. Similarly, from Figure 5b, *u* = 100 μm gives the best spectra both in terms of peak absorption and high Q factor, and there is a remarkable decrease in the absorption when the dimensions are changed further. We observe this sort of effect because when the unit cell dimension diverges a little from its optimum value of 100 μm, a mismatch occurs between the phase and magnitude preconditions, resulting in destructive interference due to numerous reflections, thereby degrading the absorption characteristics. Finally, the radius of the ring resonators is taken to be 23 μm. It is observed from Figure 5c that the absorption is maximized when the value of the radius of the metallic circular patch is 23 μm, accompanied by a relatively narrower FWHM and higher resonance frequency. Increasing the radius of the circular patch increases the area of the resonator, and the resonance shifts to a lower frequency. The opposite occurs when the radius of the circular patch is reduced.
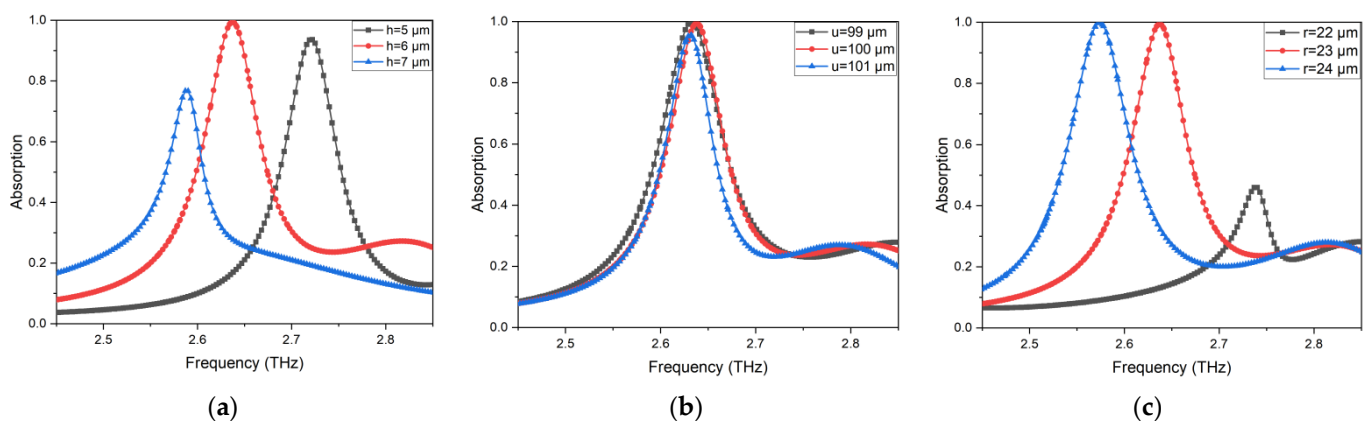

Figure 5. Parametric analysis for (**a**) thickness of the substrate; (**b**) dimension of the unit cells; (**c**) radius of the circular patches.

In the majority of the cases involving sensing applications, the encircling medium entirely encompasses the sensor, and the medium thickness is much greater than the coherent length of the light wave incident upon the sensor, which is why the medium thickness can even be considered to be infinity [33]. The variation in the absorption spectra with respect to the refractive index '*n*' is shown in Figure 6, and the variation in the peak absorption with respect to the refractive index is shown in Table 3. It is also seen that for a slight change in the refractive index of the encircling medium, there is a significant shift in the peaks of the absorption spectrum, thus indicating that the proposed design acts as an excellent refractive index sensor.

The range in which the refractive index is varied lies between *n* = 1.34 to *n* = 1.39 at an interval of 0.005. The refractive index is varied in this range because various bio-medical sensing applications are centered around a refractive index of 1.35 [34]. For instance, the blood of a healthy and fit adult exhibits a refractive index of about 1.35, while if that person gets infected by T-type leukemia, which generally occurs in the Jurkat cells, the refractive index of the blood changes to 1.39 [21]. Normally the Jurkat cells exhibit a refractive index of 1.375. Moreover, the basal cells exhibit a refractive index of 1.36 in normal conditions, but the same cell possesses a refractive index of 1.38 when it becomes cancerous [21]. Table 4 represents the various distinctive refractive indices of normal or stable and cancer-affected cells of different organs present in our body, from which it can be seen that a significant proportion of the bio-medical samples are within a refractive index range of 1.34 to 1.39. Hence, the proposed sensor can be used in applications related to bio-medical sensing.
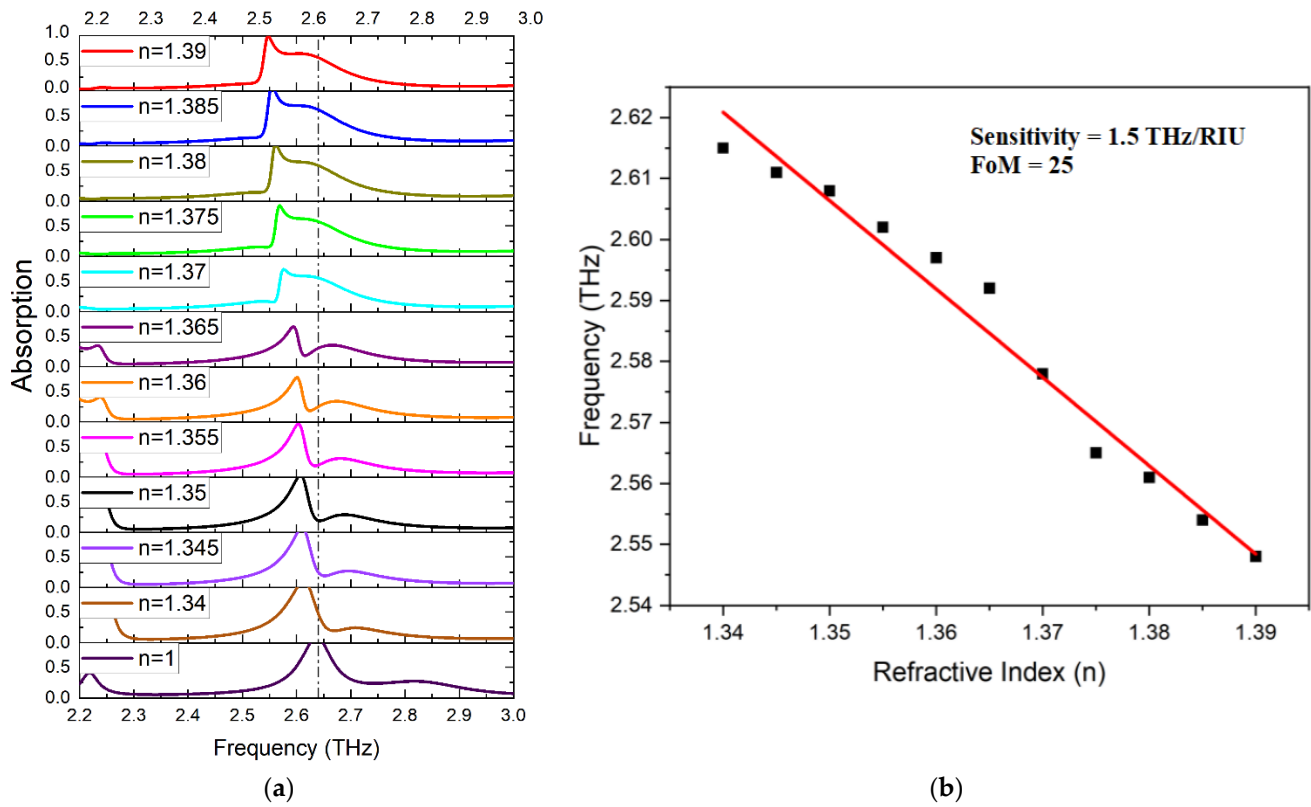
Figure 6. (**a**) Absorption spectra for different refractive indexes; (**b**) plot of the resonance frequency with respect to the refractive index.

Table 3. Variation in peak absorption with respect to the refractive index.

Refractive index	1.34	1.345	1.35	1.355	1.36	1.365	1.37	1.375	1.38	1.385	1.39
Absorption	99.99	97.25	93.14	88.0	75.0	68.0	72.0	82.0	95.0	98.5	99.99

Table 4. Refractive indices for various cells in their normal and cancerous states [35].

Cell Name	Refractive Index (*n*)
Human blood (healthy)	1.35
Basal cell (cancerous)	1.38
Basal cell (normal)	1.38
Normal breast cell (MDAMD-231)	1.385
Normal cervical cell	1.368
Jurkat (cancerous)	1.39
Jurkat (normal)	1.376
Normal breast cell (MCF-7)	1.36
PC12 cell	1.381

It can be observed from Figure 5a that as the refractive index of the material increases, the resonance frequency decreases, and vice versa. Figure 5b shows the plot of resonance frequency versus refractive indices from which the value for sensitivity is calculated. Sensitivity (*S*) can be defined as the ratio of change in the resonance frequency (f_0) to the change in the refractive index (*n*) as given in Equation (2) [27].

$$S = \frac{\Delta f_0}{\Delta n} \tag{2}$$

A linear relationship between the resonant frequency and the refractive index of the encompassing medium is obtained by curve fitting and is given by Equation (3).

$$f_0 = -1.5n + 4.674 \qquad (3)$$

Thus, the sensitivity of the proposed biomedical sensor has been found to be approximately 1500 GHz/RIU. A comparison with similar designs with biomedical applications is shown in Table 5.

Table 5. Performance comparison of the proposed sensor in terms of material used and sensitivity.

Reference	Top and Bottom Layer Metal	Total Sensitivity
[12]	Gold	163 GHz/RIU
[21]	Gold	300 GHz/RIU
[25]	Aluminum	187 GHz/RIU
[36]	Metallic SPP	1420 GHz/RIU
[37]	Aluminum	420 GHz/RIU
This Paper	Aluminum	1500 GHz/RIU

Thus, the design uses low-cost Aluminum to achieve a significant sensitivity of 1500 GHz/RIU. Another important metric used to compare sensing performances of various sensors is called the FoM, which is the ratio of the sensitivity to the FWHM of the absorber given by Equation (4) [21]. In the proposed design, the FoM was found to be 25. The proposed refractive index sensor design has a high sensitivity towards sensing bio-medical samples. Additionally, its high FoM makes it an excellent bio-medical sensor.

$$\text{FoM} = \frac{S}{\text{FWHM}} \qquad (4)$$

4. Conclusions

This paper presents a study and analysis of the design of an idiosyncratic metamaterial absorber that can be used to detect biomedical samples, especially cancer cells, in the terahertz regime. The proposed absorber is highly sensitive to alterations in the refractive index of the encompassing medium. It hence can act as an excellent refractive index sensor exhibiting a sensitivity of 1.5 THz/RIU when varied in the range of 1.34 to 1.39, due to the existence of numerous biomedical samples within this range. The sensor possesses a high Q-factor as well as an FoM of 44 and 25, respectively. Moreover, the suggested design is very simple, light-weight, and cost-effective as it uses aluminum for the top and bottom surfaces. Thus, the proposed sensor is a practical and feasible biosensor that can be used to detect biomedical samples.

Author Contributions: Conceptualization, B.A.; methodology, B.A. and A.V.J.; software, S.B., U.N. and P.D., validation, S.B., U.N. and P.D.; investigation, B.A. and A.V.J.; resources, S.B., U.N. and P.D.; data curation, S.B., U.N. and P.D.; writing—original draft preparation, A.V.J. and B.A.; supervision, N.B. and B.A.; project administration, B.A.; formal analysis: N.B.; funding acquisition: N.B.; visualization: N.B.; writing—review and editing: N.B.; figures and tables, A.V.J. All authors have read and agreed to the published version of the manuscript.

Institutional Review Board Statement: Not applicable.

Informed Consent Statement: Not applicable.

Data Availability Statement: Not applicable.

Conflicts of Interest: The authors declare no conflict of interest.

References

1. Ramakrishna, S.A.; Grzegorczyk, T.M. *Physics and Applications of Negative Refractive Index Materials*; CRC Press: Boca Raton, FL, USA, 2008.
2. Tanaka, T. Metamaterial absorbers and their applications. In *JSAP-OSA Joint Symposia*; Optical Society of America: Washington, DC, USA, 2017.
3. Kollatou, T.M.; Dimitriadis, A.I.; Assimonis, S.D.; Kantartzis, N.V.; Antonopoulos, C.S. Mulit-Band, Highly Absorbing, Microwave Metamaterial Structures. *Appl. Phys. A Mater. Sci. Process.* **2014**, *115*, 555–561. [CrossRef]
4. Rhee, J.Y.; Yoo, Y.J.; Kim, K.W.; Kim, Y.J.; Lee, Y.P. Metamaterial-Based Perfect Absorbers. *J. Electromagn. Waves Appl.* **2014**, *28*, 1541–1580. [CrossRef]
5. Appasani, B.; Prince, P.; Ranjan, R.K.; Gupta, N.; Verma, V.K. A Simple Multi-Band Metamaterial Absorber with Combined Polarization Sensitive and Polarization Insensitive Characteristics for Terahertz Applications. *Plasmonics* **2018**, *14*, 737–742. [CrossRef]
6. Verma, V.K.; Mishra, S.K.; Kaushal, K.K.; Lekshmi, V.; Sudhakar, S.; Gupta, N.; Appasani, B. An Octaband Polarization Insensitive Terahertz Metamaterial Absorber Using Orthogonal Elliptical Ring Resonators. *Plasmonics* **2019**, *15*, 75–81. [CrossRef]
7. Yen, T.J.; Padilla, W.J.; Fang, N.; Vier, D.C.; Smith, D.R.; Pendry, J.B.; Basov, D.N.; Zhang, X. Terahertz Magnetic Response from Artificial Materials. *Science* **2004**, *303*, 1494–1496. [CrossRef] [PubMed]
8. Ling, X.; Xiao, Z.; Zheng, X. Tunable terahertz metamaterial absorber and the sensing application. *J. Mater. Sci. Mater. Electron.* **2017**, *29*, 1497–1503. [CrossRef]
9. Tao, H.; Strikwerda, A.; Liu, M.; Mondia, J.P.; Ekmekci, E.; Fan, K.; Kaplan, D.L.; Padilla, W.J.; Zhang, X.; Averitt, R.D.; et al. Performance enhancement of terahertz metamaterials on ultrathin substrates for sensing applications. *Appl. Phys. Lett.* **2010**, *97*, 261909. [CrossRef]
10. Appasani, B. An Octaband Temperature Tunable Terahertz Metamaterial Absorber Using Tapered Triangular Structures. *Prog. Electromagn. Res. Lett.* **2021**, *95*, 9–16. [CrossRef]
11. Appasani, B. Temperature Tunable Seven Band Terahertz Metamaterial Absorber Using Slotted Flower–Shaped Resonator on an InSb Substrate. *Plasmonics* **2021**, *16*, 833–839. [CrossRef]
12. Cong, L.; Singh, R. Sensing with THz metamaterial absorbers. *arXiv* **2014**, arXiv:1408.3711.
13. Li, Y.; Chen, X.; Hu, F.; Li, D.; Teng, H.; Rong, Q.; Zhang, W.; Han, J.; Liang, H. Four resonators based high sensitive terahertz metamaterial biosensor used for measuring concentration of protein. *J. Phys. D Appl. Phys.* **2018**, *52*, 095105. [CrossRef]
14. Shen, F.; Qin, J.; Han, Z. Planar antenna array as a highly sensitive terahertz sensor. *Appl. Opt.* **2019**, *58*, 540–544. [CrossRef]
15. Cong, L.; Tan, S.; Yahiaoui, R.; Yan, F.; Zhang, W.; Singh, R. Experimental demonstration of ultrasensitive sensing with terahertz metamaterial absorbers: A comparison with the meta-surfaces. *Appl. Phys. Lett.* **2015**, *106*, 031107. [CrossRef]
16. Rezagholizadeh, E.; Biabanifard, M.; Borzooei, S. Analytical design of tunable THz refractive index sensor for TE and TM modes using graphene disks. *J. Phys. D Appl. Phys.* **2020**, *53*, 295107. [CrossRef]
17. Zhang, Y.; Li, T.; Zeng, B.; Zhang, H.; Lv, H.; Huang, X.; Zhang, W.; Azad, A.K. A graphene based tunable terahertz sensor with double Fano resonances. *Nanoscale* **2015**, *7*, 12682–12688. [CrossRef]
18. Yahiaoui, R.; Tan, S.; Cong, L.; Singh, R.; Yan, F.; Zhang, W. Multispectral terahertz sensing with highly flexible ultrathin metamaterial absorber. *J. Appl. Phys.* **2015**, *118*, 083103. [CrossRef]
19. Islam, M.; Rao, S.J.M.; Kumar, G.; Pal, B.P.; Chowdhury, D.R. Role of Resonance Modes on Terahertz Metamaterials based Thin Film Sensors. *Sci. Rep.* **2017**, *7*, 7355. [CrossRef]
20. AI-Naib, I. Thin-film sensing via fano resonance excitation in symmetric terahertz metamaterials. *J. Infrared Millim. Terahertz Waves* **2018**, *39*, 1–5. [CrossRef]
21. Saadeldin, A.S.; Hameed, M.F.O.; Elkaramany, E.M.; Obayya, S.S.A. Highly Sensitive Terahertz Metamaterial Sensor. *IEEE Sens. J.* **2019**, *19*, 7993–7999. [CrossRef]
22. Xie, Q.; Dong, G.-X.; Wang, B.-X.; Huang, W.-Q. High-Q Fano Resonance in Terahertz Frequency Based on an Asymmetric Metamaterial Resonator. *Nanoscale Res. Lett.* **2018**, *13*, 294. [CrossRef]
23. Yu, J.; Lang, T.; Chen, H. All-Metal Terahertz Metamaterial Absorber and Refractive Index Sensing Performance. *Photonics* **2021**, *8*, 164. [CrossRef]
24. Yahiaoui, R.; Strikwerda, A.C.; Jepsen, P.U. Terahertz Plasmonic Structure with Enhanced Sensing Capabilities. *IEEE Sens. J.* **2016**, *16*, 2484–2488. [CrossRef]
25. Banerjee, S.; Nath, U.; Shruti; Jha, A.V.; Pahadsingh, S.; Appasani, B.; Bizon, N.; Srinivasulu, A. A Terahertz Metamaterial Absorber Based Refractive Index Sensor with High Quality Factor. In Proceedings of the 2021 13th International Conference on Electronics, Computers and Artificial Intelligence (ECAI), Pitesti, Romania, 1–3 July 2021; pp. 1–4. [CrossRef]
26. Wang, B.-X.; He, Y.; Lou, P.; Xing, W. Design of a dual-band terahertz metamaterial absorber using two identical square patches for sensing application. *Nanoscale Adv.* **2020**, *2*, 763–769. [CrossRef]
27. Chen, H.T.; O'Hara, J.F.; Taylor, A.J.; Averitt, R.D.; Highstrete, C.; Lee, M.; Padilla, W.J. Complementary planar terahertz metamaterials. *Opt. Express* **2007**, *15*, 1084–1095. [CrossRef]
28. Kollatou, T.M.; Dimitriadis, A.I.; Assimonis, S.D.; Kantartzis, N.V.; Antonopoulos, C. A Family of Ultra-Thin, Polarization-Insensitive, Multi-Band, Highly Absorbing Metamaterial Structures. *Prog. Electromagn. Res.* **2013**, *136*, 579–594. [CrossRef]

29.　Li, M.; Yang, H.-L.; Hou, X.-W.; Tian, Y.; Hou, D.-Y. Perfect Metamaterial Absorber with Dual Bands. *Prog. Electromagn. Res.* **2010**, *108*, 37–49. [CrossRef]

30.　Shen, X.; Cui, T.J.; Zhao, J.; Ma, H.F.; Jiang, W.X.; Li, H. Polarization-independent wide-angle triple-band metamaterial absorber. *Opt. Express* **2011**, *19*, 9401–9407. [CrossRef]

31.　Gu, S.; Barrett, J.; Hand, T.H.; Popa, B.; Cummer, S.A. A broadband low-reflection metamaterial absorber. *J. Appl. Phys.* **2010**, *108*, 064913. [CrossRef]

32.　Bilotti, F.; Toscano, A.; Alici, K.B.; Ozbay, E.; Vegni, L. Design of Miniaturized Narrowband Absorbers Based on Resonant-Magnetic Inclusions. *IEEE Trans. Electromagn. Compat.* **2010**, *53*, 63–72. [CrossRef]

33.　Darvishzadeh, A.; Alharbi, N.; Mosavi, A.; Gorji, N.E. Modeling the strain impact on refractive index and optical transmission rate. *Phys. B Condens. Matter* **2018**, *543*, 14–17. [CrossRef]

34.　AI-Naib, I. Biomedical Sensing with Conductively Coupled Terahertz Metamaterial Resonators. *IEEE J. Sel. Top. Quantum Electron.* **2017**, *23*, 1–5. [CrossRef]

35.　Ayyanar, N.; Thavasi Raja, G.; Sharma, M.; Kumar, D.S. Photonic crystal fiber-based refractive index sensor for early detection of cancer. *IEEE Sens. J.* **2018**, *18*, 7093–7099. [CrossRef]

36.　Chen, X.; Fan, W. Ultrasensitive terahertz metamaterial sensor based on spoof surface plasmon. *Sci. Rep.* **2017**, *7*, 2092. [CrossRef]

37.　Yi, Z.; Liang, C.; Chen, X.; Zhou, Z.; Tang, Y.; Ye, X.; Yi, Y.; Wang, J.; Wu, P. Dual-Band Plasmonic Perfect Absorber Based on Graphene Metamaterials for Refractive Index Sensing Application. *Micromachines* **2019**, *10*, 443. [CrossRef]